

Atomistic Modelling of Redox Reactions in Non-Equilibrium

Wolf B. Dapp¹ and Martin H. Müser^{1,2}

¹ John von Neumann Institute for Computing (NIC), Jülich Supercomputing Centre,
Forschungszentrum Jülich, 52425 Jülich, Germany
E-mail: {w.dapp, m.mueser}@fz-juelich.de

² Department of Materials Science and Engineering, Universität des Saarlandes,
66123 Saarbrücken, Germany

We developed a new atomistic method to model (non-equilibrium) redox reaction using empirical force fields for use in MD simulations. To this end, we added the (formal) ionisation state as a discrete variable into the “split charge equilibration” method (SQE). This extension allows atoms to swap integer charges across bonds, in addition to exchanging fractional charges. We call this method “redoxSQE”, and, in first steps, used it to study contact electrification and to set up a model rechargeable nano-battery that reproduces the generic features of the discharge of a macroscopic battery qualitatively. Other popular charge-transfer force fields fundamentally cannot describe any history-dependent effect because they calculate the charge distribution as a unique function of atomic positions. For similar reasons, state-of-the-art DFT-based methods fail to describe redox reactions in non-equilibrium.

1 Introduction

Redox reactions involve a change of *oxidation state*, most commonly by exchanging an electron between a donor (which is oxidised) and an acceptor (which is reduced). Such reactions are of fundamental importance for instance in many biological processes (such as cellular respiration), but also in electrochemical cells, e.g., rechargeable batteries. Redox reactions are also at the heart of one of the oldest scientific experiments: Thales of Miletus rubbed cat-fur against a piece of amber and found that the latter becomes electrically attractive to things like wool. He sought rational explanations for this effect which we now know as triboelectricity and contact electrification. In fact, the word “electron” is the Greek word for amber. Our research group takes a top-down approach to introducing the concept of oxidation states into an atomistic empirical force-field description, by attempting to reproduce qualitatively (as an initial step) results for instance relating to battery discharge¹. Other groups² are working on deriving SQE (see Sec. 2) plus oxidation states from the bottom up, from DFT (density functional theory).

In many cases, the molecular systems of interest either contain so many atoms or evolve on such long time scales that they are beyond the reach of DFT or *ab initio*-based MD (molecular dynamics), and reasonably accurate empirical force fields are needed. Those have indeed been derived for a variety of systems, but a weak point remains the realistic handling of electrostatic interactions. Fixed-charge models are unsuitable, for example, at interfaces (e.g., a silicon dioxide layer on bulk silicon), or indeed for any other chemically heterogeneous systems, where the charge on each atom strongly depends on its chemical environment. Likewise, whenever a redox reaction occurs, the effective (fractional) charge of the participating atoms will be changed, in a quasi-discontinuous fashion. Here, we

will summarise selected recent results of our research group regarding the simulation of (non-equilibrium) redox reactions^{1,3,4}.

2 SQE and redoxSQE

The general strategy in methods that assign effective atomic charges on the fly is to minimise an energy expression (typically a quadratic expansion of the interaction between atoms) with respect to the charges. In the most popular *charge equilibration* (QE) model, also used in the so-called “reactive force field” ReaxFF⁵, the linear term involves the electronegativity, χ , while the quadratic term is proportional to the chemical hardness of atoms, κ , which reflects its charge self-interaction. In principle, atomic hardnesses and electronegativities are element-specific properties that can be obtained through finite differences from the free-atom electron affinity and the first ionisation energy. For a formal, DFT-based justification of the originally *ad hoc* introduced parameters see work by Verstraelen *et al.*^{2,6}. An alternative to QE approach is the *atom-atom charge transfer* (AACT) model⁷, which is based on the idea that charge is transferred through chemical bonds. Here, the quadratic term penalises charge transfer via a so-called bond hardness, $\kappa^{(b)}$, which is essentially inversely proportional to the polarisability of the chemical bond. The *split-charge equilibration* (SQE) model is a hybrid of these two approaches⁸. Let q_{ij} be the partial charge split between atom i and atom j , with the symmetry relation $q_{ij} \equiv -q_{ji}$. The total effective charge on atom i is given by

$$Q_i = \sum_{ij} q_{ij}, \quad (1)$$

and the expression to minimise becomes

$$V = V_C(\{\mathbf{R}, Q\}) + \sum_i \left(\frac{\kappa_i}{2} Q_i^2 + \chi_i Q_i \right) + \sum_{i,j>i} \frac{1}{2} \kappa_{ij}^{(b)} q_{ij}^2, \quad (2)$$

where $V_C(\{\mathbf{R}, Q\})$ is the Coulomb energy, which depends both on the atomic and the charge configuration. The bond hardness $\kappa_{ij}^{(b)}$ depends on the types of atoms forming the bond *and* on their separation. The QE model arises in the limit where all $\kappa^{(b)}$ are set to zero (i.e., the system is infinitely polarisable), while AACT is equivalent to neglecting the atomic κ .

Both QE and AACT fail to reproduce certain generic trends. For example, AACT does not show the proper scaling of the polarisability for oligomers⁹ in the limit of small degrees of polymerisation P , and the skin depth for external fields in solids is always less than an atomic spacing¹⁰. Furthermore, it fails to describe metals, or any material with a dielectric constant not ≈ 1 . Conversely, dielectric behaviour is ruled out in QE, and solids always behave as ideal metals¹⁰. Moreover, polar molecules show the wrong scaling of the polarisability⁹ and dipole¹¹ for long-chained polymers. Finally, because of its polarisability, QE also produces the wrong dissociation limit of molecules. For example, if a CH_4 molecule were separated from an H_2O molecule, the molecules would carry nonphysical charges of about $\pm 0.4 e$, where e is the elementary charge, unless artificial constraints were imposed. None of these artifacts arise with SQE.

However, like its competitors, the original formulation of SQE still fails to describe true ions. In a realistic parameterisation the bond hardness diverges once orbitals between

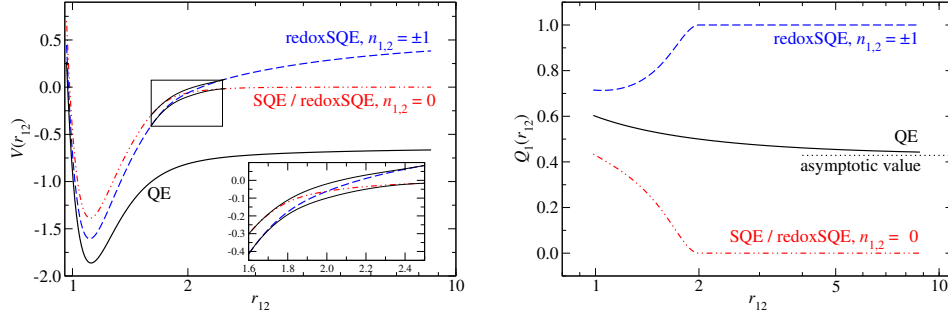


Figure 1. From Ref. 3. In both graphs, two different oxidation state configurations are considered as well as the conventional charge equilibration approach (QE). **Left:** energy V_{12} of a (generic) diatomic molecule as a function of the interatomic distance. The thick black lines in the inset sketch the behaviour of the energy of the quantum-mechanical ground state and the first excited state. The SQE model violates the non-crossing rule unlike the true, quantum-mechanical ground state. This makes the SQE system evolve according to diabatic dynamics, unless the oxidation numbers are altered during a reaction. **Right:** fractional effective charge Q_1 of the “cation” with different methods. The dotted black line is the charge on the electropositive atom predicted by the QE method for an infinite separation.

neighbouring atoms no longer overlap at large interatomic distances. Then electropositive atoms automatically cease to donate their electrons to electronegative atoms, and both partners are neutral. This shortcoming is remedied with the introduction of a (formal) oxidation state as a variable⁴. We modify Eq. 1, and now calculate the charge according to

$$Q_i = \sum_{ij} q_{ij} + n_i e, \quad (3)$$

where n_i is an integer number. The oxidation state can be thought of as excess integer charges on atom i . Note that no bond-related energy penalty applies when *integer* charges are moved about the system.

The concept of formal (integer) oxidation numbers makes it possible to simulate charging or discharging of Galvanic cells, or, more generally, any type of processes involving redox reactions, as well as electrostatic fields of zwitterionic molecules, which violate the principle of local charge neutrality. Moreover, the partial charge of an atom can now be made history dependent because, for any given atomic configuration, the system can assume a number of different minima of V , one for each unique $\{n_i\}$ configuration, akin to Landau-Zener levels.

The oxidation state dynamics can be parameterised so that it mimics a Landau-Zener process. The dynamics can involve “radiation”, i.e., a discontinuous (energy) change of the system. This could happen because the new oxidation state of the system necessitates a reoptimisation of all split charges. Alternatively, radiation-free redox reactions are possible either if the excess energy is supplied to the system as kinetic energy, or if the redox reaction happens exactly at $q_{ij} = e/2$. Radiation-free redox reactions play an important role in Marcus theory¹², which was the first generally accepted theory of electron transfer. Fig. 1 shows for the dissociation of a generic diatomic molecule energy levels and charge evolution as a function of separation.

In our implementation, a stochastic process determines for a specific bond whether we

attempt an integer charge transfer move. A Metropolis-type criterion on the energy decides whether such a trial move across a dielectric bond (i.e., one having non-zero bond hardness) is accepted or rejected. Similar to Tully surface hopping¹³, an integer charge transfer takes the system to a different Landau-Zener level on which it will evolve subsequently. An integer charge transfer across a metallic bond is always accepted, because the bond hardness and therefore the change in energy during a trial move is zero – the integer charge transfer is perfectly balanced by the transfer of partial charge between the participating atoms.

We calculate the bond hardness as a divergent rational function according to the (heuristic) formula

$$\kappa_{ij}^{(b)} = \begin{cases} \kappa_{ij}^{(p)} & r_{ij} \leq r_s, \\ \kappa_{ij}^{(p)} + \kappa_{ij}^{(0)} \frac{r_1^2 (r_{ij} - r_s)^2}{r_s^2 (r_1 - r_{ij})^2} & r_s < r_{ij} < r_1, \\ \infty & r_1 \leq r_{ij}, \end{cases} \quad (4)$$

where $\kappa_{ij}^{(p)}$ is a plateau value ($\equiv 0$ for metals), $\kappa_{ij}^{(0)}$ is a bond-specific parameter, and r_s and r_1 are short- and long-separation cutoffs, respectively. This expression has been shown¹⁴ to work well for fractional charges in the homolysis of a variety of organic molecules, even for some radicals and transition states although the calibration was done on equilibrated structures satisfying the octet rule. The long-range cutoff is convenient for computational reasons.

In the following, we briefly discuss two applications of the *redoxSQE* method: (i) to contact electrification, and (ii) to battery discharge. For more details, we refer the reader to the original literature^{1,3,4}.

3 Contact Electrification

If two neutral solids (e.g., gold and sodium) are brought into contact, charge transfers between them, and, upon separation, they retain some of that charge. This means that after contact formation there is an electrostatic attraction between the clusters that was not there before – even if one assumes an identical atomic configuration before and after. Such history dependence is not captured by most charge-transfer force fields. They determine fractional charges as a unique function of the instantaneous atomic positions just like conventional DFT computes a unique charge density for a given atomic configuration.

For metals, the mechanism of contact electrification is well established¹⁵. Electrons transfer from the metal having the smaller work function to that with the larger one. The precise *amount* of transferred charge is affected by electrostatics, e.g., by the total capacitance of the metals and by the rate at which the two solids are pulled apart. Nevertheless, the *direction* of charge flow between initially neutral metals is entirely determined by their work functions.

The rubbing-induced charge transfer between dielectrics is much less well understood. Electron transfer¹⁶, proton transfer¹⁷, or the exchange of hydroxide or other ions¹⁸ have all been suggested as the possible origin of contact-dynamics-induced charging. Unlike metals, dielectrics cannot be arranged into a linear triboelectric series in an unambiguous fashion, sometimes the series is even cyclic. For example, during rubbing with the material

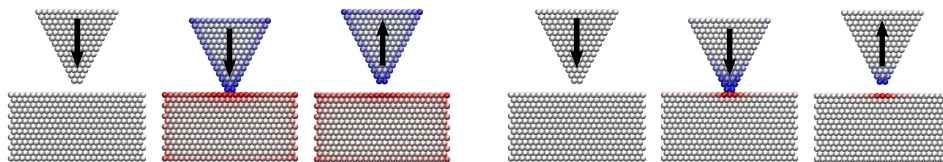


Figure 2. From Ref. 3. **Left:** visualisation of the contact electrification of a metal tip and a metal substrate. Red and blue indicate, respectively, the amount of negative and positive charge on an atom. Initially neither solid is charged. When they are brought to close proximity, charge can pass between them such that negative charge flows from the metal with the smaller work function to that with the larger work function. The charge distribution mainly lives on the surface of the clusters, as expected for metals, because this minimises the (repulsive) electrostatic energy. After the solids have been separated, no more charge can flow. With redoxSQE, both solids retain a constant, integer charge, while AACT predicts that both parts will be neutral again after separation. With DFT or QE, neither parts can be neutral at any point (not even during the approach), as charge is transferred non-locally and over arbitrary distances with those schemes. **Right:** Similar, except that here the bonds within each solid are modelled as dielectric. This prevents the charge from spreading across the solids’ surfaces. Also, the total transferred (integer) charge is smaller than for metals.

an entry further left each material in the list {glass, zinc, silk, filter paper, cotton, glass} gains negative charge¹⁹.

Fig. 2 demonstrates that our model reproduces the qualitative features of contact electrification for *both* cases. In the original publication³, we show a number of model systems, including the contact between two metal clusters, two dielectric solids, and the dissociation of an NaCl dimer. For the latter case, we also performed quantum-chemical calculations to show that the method can be adapted to fit a real system. In this case, the first of two possible outcomes is that the dimer breaks up to form two neutral products (as in fact all diatomic molecules do with the exception of FrCl). This happens in an inert environment, such as an argon atmosphere. QE – and likewise currently used approximations to the exact DFT functionals – incorrectly predict a remnant charge of $\approx \pm 0.5$ e on the atoms at infinite distance in this case (see also Fig. 1). Conversely, in a sufficiently polar environment (e.g., an NaCl dimer surrounded by ≥ 4 water molecules), the dimer dissociates as the ions Na^+ and Cl^- . RedoxSQE can reproduce both cases, as well as the energy curves and the ESP (electrostatic potential) partial charges with respect to the separation³.

The physical concept behind redoxSQE is that the oxidation state is largely independent of the instantaneous atomic configuration. This allows for history dependence in that the system can evolve on, and switch between, different, independent Landau-Zener levels. The oxidation state is a discrete quantity and a change involves a redox reaction implicating two or more nearby atoms. The effective total charges are determined anew after each transfer of integer charge.

4 Towards Modelling a Battery Atomistically

Battery research and development has been experiencing a tremendous surge in recent years, as it is crucial to overcome technological challenges related to energy production (e.g., buffering output peaks of renewable energy power plants), storage (e.g., for use in portable electronic devices) and usage (e.g., for automotive purposes). In a model system more complex than contact electrification, we took first steps towards modelling a battery

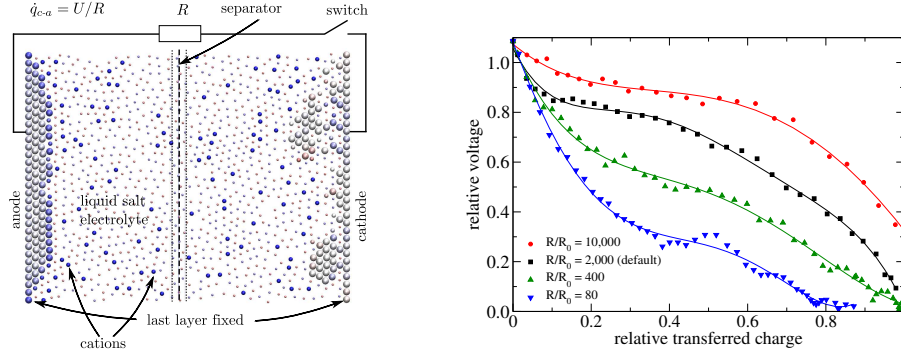


Figure 3. From Ref. 1. **Left:** illustration of a battery setup with 1194 atoms. Charge is encoded in the colouring: blue means positive, red negative charge. For visual distinction, (fixed-charge) electrolyte particles are chosen smallest, independent of their LJ radii, and their charge colouring is halved. The medium-sized particles are cations, while the largest particles are metallic atoms. The separator (salt bridge) keeps non-electrolyte atoms from moving between the two half-cells but lets electrolyte atoms pass. A resistive external load R (following Ohm's law) completes the circuit. **Right:** Discharge curves of our battery demonstrator with different external resistors. The data represents an average over 4 independent runs, and each point is averaged over many MD time steps. The solid lines are inserted to guide the eye. The higher the external resistance, the closer the battery's behaviour approaches an ideal discharge curve, the lower the load, the more the internal resistance dominates. In this property, and the shape of the discharge curve, our nano-battery resembles a macroscopic battery. Initially, the voltage declines sharply, as the electrodes are charged before ions are dissolved or adsorbed, respectively. This is followed by an extended plateau when the voltage stays constant as the charge transfer through the external resistance is balanced by an equal amount of ion transfer in the electrolyte. At the same time, additional charge on the electrodes is now compensated by dissolving and adsorbing ions. Finally, another steep decline concludes the discharge, as the electrodes are consumed and their surfaces passivated.

as a whole¹, atomistically. This attempts to fill a gap between mesoscopic porous electrode models^{20,21} commonly used for commercial battery applications on the one hand, and DFT- or MD-based simulations of isolated and specialised aspects of individual processes²² happening in a half-cell on the other hand.

We set up a system that resembles a traditional Voltaic wet-cell, containing two metal electrodes, a liquid electrolyte (which we model as purely ionic), an adjustable Ohmic external load, and a salt bridge that keeps the electrodes from touching (which would create a short circuit), but allows electrolyte ions to pass. The short-range interaction is calculated with a Lennard-Jones (LJ) potential, and the electrolyte is modelled as a Kob-Andersen glass in order to avoid freeze-out. Fig. 3 (left panel) illustrates the setup. When the switch is closed, the difference in chemical potential between the two electrodes drives a current through the external load. The circuit is completed by electrolyte ions streaming from one half-cell to the other. In contrast to other charge transfer force fields, redoxSQE does not *equalise* the chemical potential between the electrodes. Instead, the method maintains a differential in chemical potential by allowing anode metal ions to be reduced and dissolve as cations. At the same time, cations adsorb to the cathode surface, are oxidised and take on the excess electrons as the second half-reaction to a full redox reaction. The process halts once the redox-active material is exhausted, i.e., the anode is dissolved and all cations have been oxidised at the cathode.

RedoxSQE also reproduces the polarisation charges naturally without having to intro-

duce explicit mirror charges. A Helmholtz double layer of electrolyte ions forms at both electrode interfaces where the potential drop occurs. In fact, one of the advantages of the method is that it allows to study the processes occurring at the electrolyte-electrode interface, also including clustering and dendrite formation.

Fig. 3 (right panel) shows the discharge behaviour for different external loads. Despite not having parameterised the simulation for any particular material but having chosen typical generic values for the free parameters, the results resemble the discharge curves of commercial batteries²³. Other macroscopic properties of battery discharge are also reproduced, such as a strong temperature dependence of capacity and available voltage, voltage recovery if the battery is allowed to relax (as happens in pulsed-discharge applications), as well as a voltage overshoot when the battery is charged. These generic features are largely independent of the parameterisation details, which hints at the transferability of the method.

In future work we will parameterise the model for specific materials of practical relevance, and improve the efficiency of the implementation so that we can model sufficiently large ensembles. However, the initial results are already quite encouraging first steps towards an atomistic model of a battery as a whole.

5 Summary

RedoxSQE can be made part of empirical force fields to model (non-equilibrium) redox reactions as they occur in problems of contact electrification and tribo-electricity as well as in electrochemical processes such as the discharge of a battery. It outperforms other charge-transfer force fields in that it does not suffer from their shortcomings, and is transferable.

We showed that redoxSQE is able to simulate processes that occur in contact electrification, although descriptions are still at a rather generic level. In principle, it can handle both metallic and dielectric contacts, and so may contribute to the debate how tribo-charging works between dielectrics.

We also demonstrated that a model battery robustly reproduces generic features seen in macroscopic battery discharge such as dependence on temperature or external load, and relaxation and recharge behaviour. Once parametrised in a material-specific way, redoxSQE can be particularly useful in studying the processes near the interface of electrolyte and electrode. It is the first empiric approach to model an entire battery atomistically. For more details, we refer the reader to the original literature^{1,3,4}.

Acknowledgements

The authors gratefully acknowledge computing time on JUROPA.

References

1. W. B. Dapp and M. H. Müser, *Redox reactions with empirical potentials: Atomistic battery discharge simulations*, J. Chem. Phys., **139**, 064106, 2013.
2. T. Verstraelen, P. W. Ayers, V. Van Speybroeck, and M. Waroquier, *ACKS2: Atom-condensed Kohn-Sham DFT approximated to second order*, J. Chem. Phys., **138**, 074108–19, 2013.

3. W. B. Dapp and M. H. Müser, *Towards time-dependent, non-equilibrium charge-transfer force fields*, Eur. Phys. J. B, **86**, 337, 2013.
4. M. H. Müser, *The chemical hardness of molecules and the band gap of solids within charge equilibration formalisms Towards force field-based simulations of redox reactions*, Eur. Phys. J. B, **85**, 135, 2012.
5. A. C. T. van Duin, S. Dasgupta, F. Lorant, and W. A. Goddard, *ReaxFF: A reactive force field for hydrocarbons*, J. Chem. Phys. A, **105**, 9396–9409, 2001.
6. T. Verstraelen, P. Bultinck, V. Van Speybroeck, P. W. Ayers, D. Van Neck, and M. Waroquier, *The Significance of Parameters in Charge Equilibration Models*, J. Chem. Theory Comput., **7**, 1750–1764, 2011.
7. R. Chelli, P. Procacci, R. Righini, and S. Califano, *Electrical response in chemical potential equalization schemes*, J. Chem. Phys., **111**, 8569–8575, 1999.
8. R. A. Nistor, J. G. Polihronov, M. H. Müser, and N. J. Mosey, *A generalization of the charge equilibration method for nonmetallic materials*, J. Chem. Phys., **125**, 094108, 2006.
9. G. L. Warren, J. E. Davis, and S. Patel, *Origin and control of superlinear polarizability scaling in chemical potential equalization methods*, J. Chem. Phys., **128**, 144110, 2008.
10. R. A. Nistor and M. H. Müser, *Dielectric properties of solids in the regular and split-charge equilibration formalisms*, Phys. Rev. B, **79**, 104303, 2009.
11. P. T. Mikulski, M. T. Knippenberg, and J. A. Harrison, *Merging bond-order potentials with charge equilibration*, J. Chem. Phys., **131**, 241105, 2009.
12. R. A. Marcus, *Chemical + electrochemical electron-transfer theory*, Ann. Rev. Phys. Chem., **15**, 155, 1964.
13. J. C. Tully, *Molecular Dynamics with electronic transitions*, J. Chem. Phys., **93**, 1061–1071, 1990.
14. D. Mathieu, *Split charge equilibration method with correct dissociation limits*, J. Chem. Phys., **127**, 224103, 2007.
15. J. Lowell and A. C. Rose-Innes, *Contact Electrification*, Adv. Phys., **29**, 947, 1980.
16. C. M. Mate, *Tribology on the small scale*, Oxford University Press, Oxford, 2008.
17. A. F. Diaz and R. M. Felix-Navarro, *A semi-quantitative tribo-electric series for polymeric materials: the influence of chemical structure and properties*, J. Electrostatics, **62**, 277–290, 2004.
18. L. S. McCarty and G. M. Whiteside, *Electrostatic Charging Due to Separation of Ions at Interfaces: Contact Electrification of Ionic Electrets*, Angew. Chem. Int. Ed., **47**, 2188–2207, 2008.
19. W. R. Harper, *Contact and frictional electrification*, Laplacian Press, Morgan Hill, 1998.
20. M. Doyle, T. F. Fuller, and J. Newman, *Modeling of galvanostatic charge and discharge of the lithium polymer insertion cell*, J. Electrochem. Soc., **140**, 1526–1533, 1993.
21. C.-W. Wang and A. M. Sastry, *Mesoscale modeling of a Li-ion polymer cell*, J. Electrochem. Soc., **154**, A1035–A1047, 2007.
22. M. Saiful Islam, *Recent atomistic modelling studies of energy materials: batteries included*, Phil. Trans. R. Soc. A, **368**, 3255–3267, 2010.
23. Procter & Gamble, “Duracell Alkaline-Manganese Dioxide battery technical bulletin”, 2012, Online; accessed on Nov 19, 2012.